

DEVELOPMENTS IN HEAVY TRANSPORT DESIGN CALCULATIONS

M.J.A. van Exsel MSc and J.B. de Jonge MSc, Dockwise, The Netherlands

SUMMARY

With continuous development in the Oil&Gas industry, there is an increase of transports of heavier and bigger structures. As these transports tends to reach the structural limits of heavy transport vessels there is a growing demand to perform more detailed transport analyses.

The paper addresses developments in heavy transport design calculations from a theoretical and an operational perspective. Both view-points contribute to a more detailed analysis of the transports and increase the safety level. Theoretical developments of design calculations are achieved by means of a so-called “Global Hull Analysis”. An integrated finite element model of the transport vessel and cargo ensures that the stiffness interaction between both is accurately represented. Hydrodynamic analysis –combined with the “design wave approach” – is performed to determine critical load cases, containing hull pressures and accelerations. These load cases are input for structural analysis to determine stresses in and support loads between cargo and heavy transport vessel.

Developments on the operational side are achieved by means of a fleet wise motion monitoring project gathering motion and weather data. This project increases insight in operational margins during transports. Concluded is that the recorded nowcast significant wave height from almost 1.200.000 nm of data hardly ever exceeds 5.0 [m], giving a significant operational margin for high design sea-states, typically $H_s > 7.0$ [m]. For low design sea-state the margin is small. The aim is to reach a constant operational margin by increasing the design sea-state at the lower range and reducing the design sea-state at the higher range. This will be implemented in a new design method.

NOMENCLATURE

CoG	Center of Gravity
CSM	Cargo Securing Manual
DW	Dockwise
ETLP	Extended Tension Leg Platform
FEM	Finite Element Method
GHA	Global Hull Analysis
GHS	General Hydrostatics
GWS	Global Wave Statistics
HTV	Heavy Transport Vessel
RAO	Response Amplitude Operator
SPOS	Ship Performance Optimization System
UC	Unity check
WSF	Wave Shear Forces
WBM	Wave Bending Moment
x acc	longitudinal acceleration
y acc	transverse acceleration

1. INTRODUCTION

Developments in heavy transport design conditions from theoretical as well as operational perspective are described. Improvements are gained by a more detailed calculation method, which is here defined as theoretical improvement.

A weather and motion monitoring project on the Dockwise fleet of vessels leads to operational improvements. Interesting insights are given from the extensive amount of data, gathered in a period of four years. Both theoretical as operational improvements lead to more insight and more accurate analyses in the heavy transport engineering.

2. GLOBAL HULL ANALYSIS

For transports of large structures, especially where deflection of the heavy transport vessel or cargo may be of importance, it is appropriate to perform extended structural analyses with loads defined by hydrodynamic analysis. This development in design calculations is called a “Global Hull Analysis”.

In this chapter the GHA method is described including a comparison between the results obtained via the conventional rigid-body calculation method and the results obtained with this more detailed GHA.

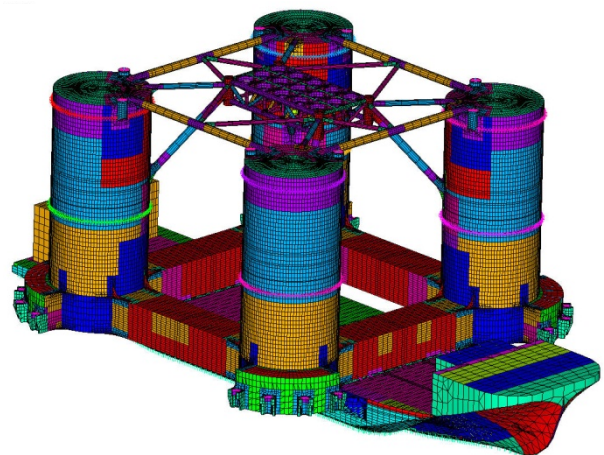


Figure 1: FE model of combined HTV and cargo

2.1 BACKGROUND

For standard analyses an in-house program is used to calculate the design parameters for the transports of large structures on heavy transport vessel. Several assumptions are made to simplify the calculations:

- Cargo and vessel are treated as rigid body
- Beam model to represent heavy transport vessel in calculation of shear and still-water bending moment
- Cribbing pressure calculations based on rigid body cargo and HTV
- Cribbing pressure in 4 points, i.e. FWD, AFT, PS & SB extreme fibers of the cribbing arrangement, see Figure 2

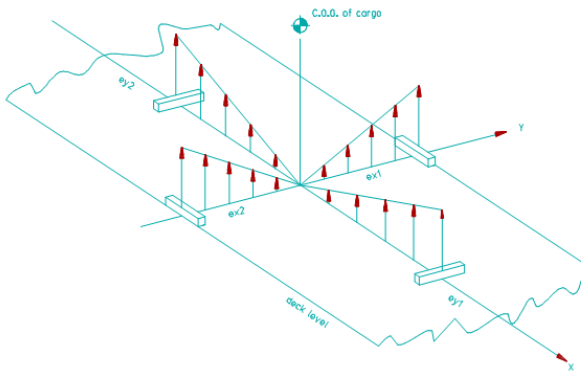


Figure 2: Cribbing pressure determination conventional method

To compensate for the simplifications as described above, the maximum allowable cribbing pressure from the conventional rigid-body method are set to 20 [kg/cm²]. This gives additional margin and makes the program suitable for most transports of large structures on a heavy transport vessel.

However, with continuous development in the Oil & Gas industry, the amount of transports of heavier and bigger structures increases. As these transports tend to reach the structural limits of the HTV, there is a growing demand to perform more detailed transport analyses to verify the structural integrity of the HTV and the cargo. Especially with large overhanging- or lengthy cargoes, which are supported over a large part of the vessels deck, stiffness interaction between cargo and HTV can have a significant impact on the design calculations.

2.2 GHA METHOD

Often overall accelerations are applied to the FE model, sometimes with a simplified method to account for wave load deflection of the HTV. For such a simplified method the relation between acceleration components and wave loads is ignored and assumptions are made. A more appropriate method is to apply hydrodynamic loads directly from 3D-diffraction software to an FE model; hydrodynamic loads consist of pressures over the underwater hull and accelerations in the system CoG.

In the FE-analysis a set of element pressures and accelerations in the center of gravity are given as input, representing global loads, where pressure and acceleration are directly correlated because phasing between the accelerations and the wave is included.

The hydrodynamic analysis is performed using the so-called “diffraction” method, which is incorporated in AQWA-Line. The AQWA-Suite of programs is capable of determining wave shear and bending and to export wave loads on the wetted surface for structural analysis. The structural analysis is performed using a FE package.

For the determination of loads for FEM the following basic steps are made:

- Based on the construction plans, loading condition and the weight distribution of the vessel and cargo, a 3-D FE Model is prepared, see Figure 1. From this FE Model, the mass, centre of gravity and the radii of gyration are calculated. With the mass data and the AQWA model, diffraction calculations are carried out, determining all action- (wave) and reaction-forces (added mass and damping). With the overall added mass, damping and wave forces and moments, the hydrodynamic response (the six motion components and their phase angles) of the vessel in waves is determined.
- Based on these results wave shear force (WSF) and bending moment (WBM) characteristics or force- and moment-characteristics between Cargo and HTV - generally called splitting forces and moments - are determined.
- Based on frequency domain analysis splitting forces and moment design values are determined. In addition linear combinations of splitting force RAO's are produced and processed to determine cribbing pressure and stress in transverse sections.
- Based on the maximum splitting forces, the most severe wave spectrum and directions are defined.
- A regular wave representing equal and comparable splitting forces is selected and used as input for AQWA-wave. This selection process is generally known as the “regular design wave approach”.
- Load-sets are created and transferred to FEM.
- Structural analysis is performed to check the integrity of cargo and HTV and to determine cribbing pressures and deflections of the HTV.

2.3 VALIDATION

A comparison of the results obtained with the conventional rigid-body method and the results obtained with the more detailed GHA are presented in this paragraph.

2.3(a) Test case description

Two transports have been selected as test cases to investigate the influence of the more detailed GHA on the design parameters for larger structures onboard heavy transport vessels.

First test case is the transport of an extended tension leg platform, ETLP, stowed onboard an HTV, see Figure 1. A GHA is performed for this transport due to the fact that weight of the ETLP is close to the limits of the HTV carrying capacity in combination with a large overhang of the ETLP on both sides of the vessel. It has to be noted that a shaped cribbing design is used for this transport. With a shaped cribbing the static cribbing pressure will be equally divided over the vessel width by adapting the cribbing height. The conventional rigid-body method uses two rigid-bodies to determine the cribbing pressure for which the results shall correspond to a shaped cribbing design. Furthermore, the HTV will be equipped with four sponsoons to increase the support area of the ETLP.

Second selected test case is the transport of a semi-submersible longitudinally stowed onboard an HTV, see Figure 3. Due to the longitudinal stowage, there is a significant contact area in longitudinal direction of the vessel. A GHA has been performed to investigate the impact of stiffness interaction between cargo and HTV. Strength of HTV is not an issue.

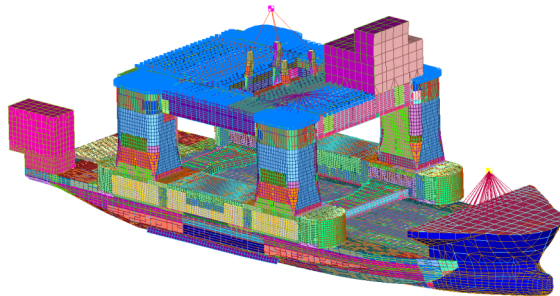


Figure 3: Combined FE model of a Heavy transport vessel and a semi-submersible longitudinally stowed

2.3(b) Validation criteria

The following design criteria are compared:

- Cribbing pressures
- Stillwater longitudinal strength of heavy transport vessel
- Deflections of heavy transport vessel

2.3 (c) Cribbing pressures validation

The limit for soft wooden cribbing pressure calculation based on the conventional rigid-body method is set at 20 [kg/cm²]. This limit contains a margin to compensate for the simplifications in the calculation method. Since fewer assumptions are made in the GHA, the allowable limits for this analysis are increased to 32 [kg/cm²] for soft wooden cribbing.

Cribbing pressures calculated for test case 1 using the rigid-body method are presented in Table 1. Table 1 contains the actual calculated cribbing pressures for both the static as well as the static + dynamic situation based on the method as briefly described in

paragraph 3.1. The cribbing pressures are converted to Unity Checks, U.C. to be able to compare them with the results of the GHA.

Table 1: Cribbing pressures test case 1

Item	Support pressures ETLP (Test case 1)			
	PS (ex1) (kg/cm ²)	SB (ex2) (kg/cm ²)	FWD (ey1) (kg/cm ²)	Aft (ey2) (kg/cm ²)
Static	11.85	11.39	11.62	11.62
Static + dynamic	20.26	19.80	16.08	16.12
Item	Support pressures HTV (Test case 1)			
	PS (ex1) (kg/cm ²)	SB (ex2) (kg/cm ²)	FWD (ey1) (kg/cm ²)	Aft (ey2) (kg/cm ²)
Static	0.59	0.57	0.58	0.58
Static + dynamic	1.01	0.99	0.80	0.81

Cribbing pressures calculated using the GHA are presented in Figure 4 & 5. Figure 4 presents the actual calculated cribbing pressure and Figure 5 presents these pressures converted to U.C.'s based on an allowable cribbing pressure limit of 32 [kg/cm²].

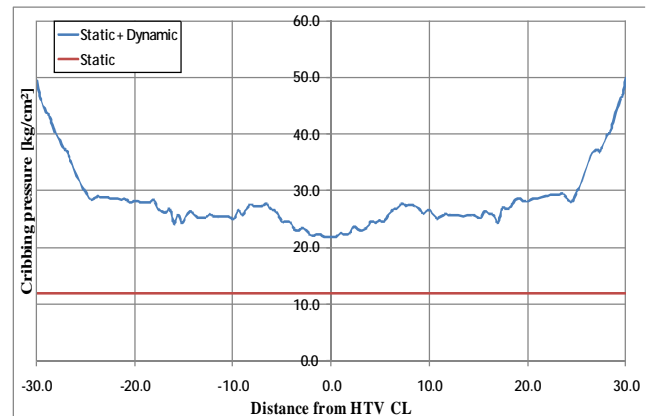


Figure 4: Cribbing pressures [kg/cm²] test case 1

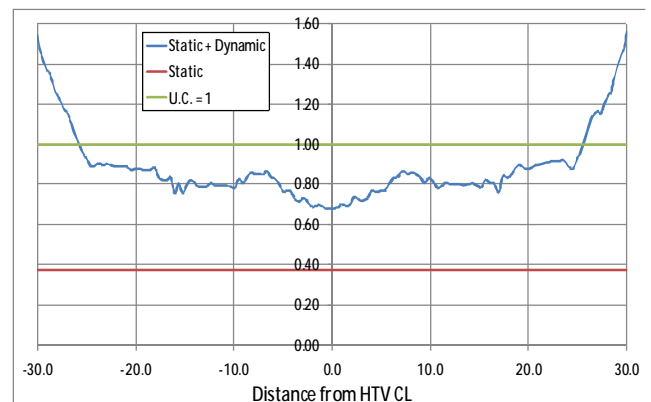


Figure 5: Cribbing pressures test case 1 converted to U.C. [-]

After comparing the cribbing pressure results of the first test case for both methods the following is noted:

- The influence of the weight distribution and the stiffness of the cargo and HTV results in significant discrepancies between the calculated cribbing pressures of both methods.

- As result of the shaped cribbing as used in the FEM analysis the static cribbing pressure is found to be uniform and similar for both methods.
- For the static + dynamic load case the difference between the two methods is found to be significant. Especially the calculated cribbing pressures below the columns are much higher for the GHA in comparison to the ones calculated by the conventional rigid-body method.

The benefit of the more detailed GHA with respect to cribbing pressure calculation is proven to be essential for this test case. Due to the non-uniform load distribution of the cargo over the width of the vessel, cribbing pressures below the columns are exceeding the allowable limits showing the need of additional cribbing wood. This could not have been obtained from the calculated cribbing pressures for the conventional rigid-body method. In addition it shows that shaped cribbing is required to guarantee a uniform load distribution in the static case.

Table 2 contains the cribbing pressures and unity check for test case 2 calculated using the conventional rigid-body method.

Table 2: Cribbing pressures test case 2

Item	Support pressures Semi (Test case 2)			
	PS (ex1) (kg/cm ²)	SB (ex2) (kg/cm ²)	FWD (ey1) (kg/cm ²)	Aft (ey2) (kg/cm ²)
Static	10.24	10.60	10.81	10.04
Static + dynamic	15.81	16.17	15.40	14.61
	PS (ex1) (kg/cm ²)	SB (ex2) (kg/cm ²)	FWD (ey1) (kg/cm ²)	Aft (ey2) (kg/cm ²)
Static	0.51	0.53	0.54	0.50
Static + dynamic	0.79	0.81	0.77	0.73

Figure 6 & 7 present the cribbing pressures calculated using the GHA method. First Figure shows the actual cribbing pressure while Figure 7 shows the cribbing pressure converted to a unity check.

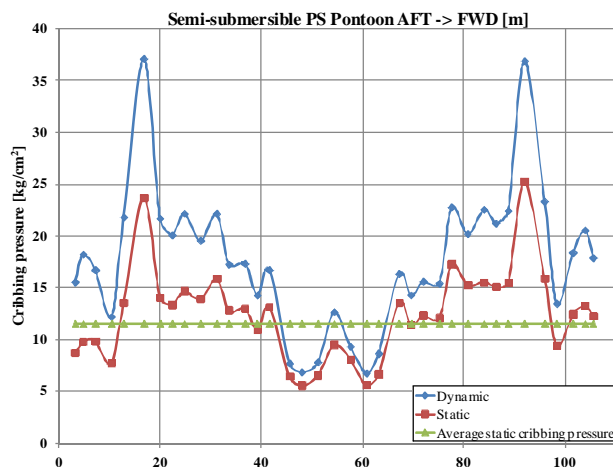


Figure 6: Cribbing pressures [kg/cm²] test case 2

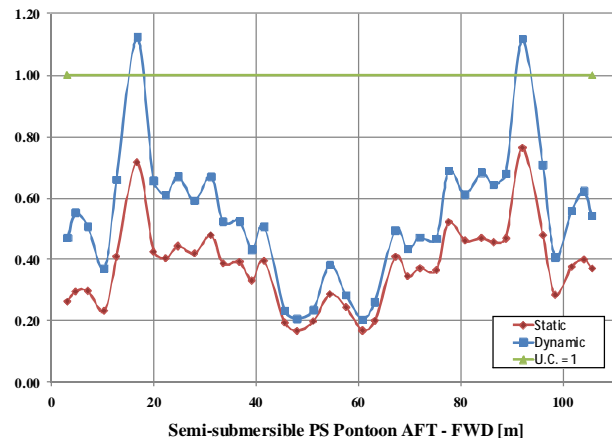


Figure 7: Cribbing pressures test case 2 converted to UC.

Based on the cribbing pressure results for test case 2, the following is noted:

- Static cribbing pressures are not similar since weight distribution along pontoon has significant influence on GHA results
- A peak in the cribbing pressures is calculated by the GHA method. This high cribbing pressure occurs in a cribbing beam which is located between a transverse bulkhead in cargo and HTV.
- Neglecting the peak pressure calculated by the GHA, the maximum U.C.'s for both calculation methods are in the same range.

Based on these two test cases, the value of having a more detailed GHA method on top of the current existing rigid-body method is proven for cribbing pressure determination. Especially for large overhanging cargoes, or cargoes with a non-uniform load distribution, the calculated cribbing pressures with the GHA method can significantly differ from the ones determined by the conventional rigid-body method. It must be noted that, due to the large margins which are taken into account in the rigid-body method, design criteria calculated by the rigid-body method with respect to cribbing pressures will be sufficient in most cases.

2.3 (d) Longitudinal strength validation

Generally for each loading Condition the still water bending moment and shear force is checked to ensure that the strength requirements of the Classification Societies, i.e. allowable vertical shear and longitudinal bending moment are met.

The shear force curve is calculated by combining the weight and buoyancy distribution over the HTV's length. Division by the sectional shear area results in the shear stresses distributed over the length of the HTV. Integration of the shear force curve over the length of the HTV results in the still-water bending moment distribution. Minimum and maximum bending moment occur at the section with zero shear load.

Maximum allowable shear force and bending moment in conventional rigid-body method are defined as a percentage of the total shear and bending. The method reserves a part of the capacity which is required for wave shear and bending contribution.

Figure 8 shows the still-water bending moment and shear force curve for test case 1 determined by the conventional rigid-body method. In this graph also the bending moment and shear force limits are presented. Shear force is close to its limits just in front and aft of both pontoons of the ETLP.

Figure 9 shows the shear stress distribution for the static condition over the different longitudinal members calculated by the GHA. Comparing the shear stress distribution with the shear force strength graph of Figure 8 it can be concluded that the trend in longitudinal direction of the HTV is similar. The shear force in the FE model is also determined just aft the aft pontoon of the ETLP (looking from stern) being 6847mt. This means that a difference of about 2% occurs between the two methods. It is concluded that in this case stiffness interaction does not have a significant influence on the calculated maximum shear force. Benefit of the FE model is that it shows the distribution over the different longitudinal members where the rigid-body cannot make a distinction between those members.

Bending stress in main deck and bottom of the HTV are presented in Figures 10 and 11. The trend in longitudinal direction is similar to the bending curve as presented in Figure 8.

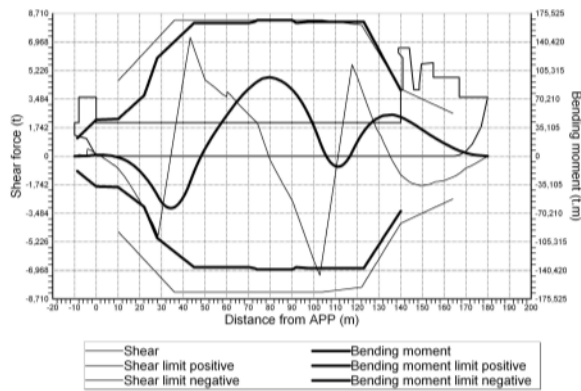


Figure 8: Still-water bending moment and shear curve

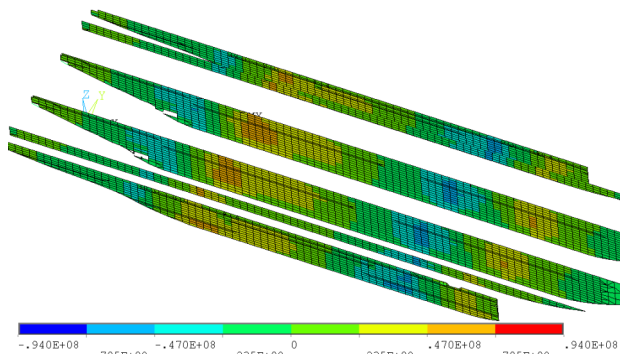


Figure 9: Shear stress in longitudinal HTV members for the static condition

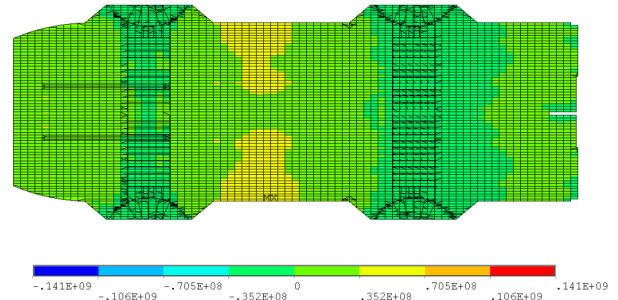


Figure 10: Bending stress in main deck of HTV for the static condition

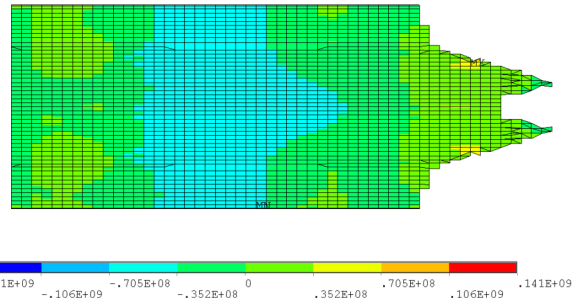


Figure 11: Bending stress in HTV bottom hull for the static condition

Figures 12 to 15 present the same graphs for test case 2 as reported above for test case 1. These figures prove that this case was not selected due to HTV strength but to investigate stiffness interaction between cargo and HTV and cribbing pressures. Stresses, as well as shear force and bending moment are fluctuating around zero not coming close to its limits.

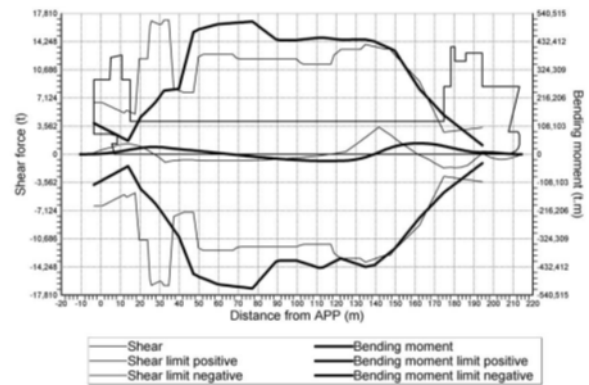


Figure 12: Still-water bending moment and shear curve

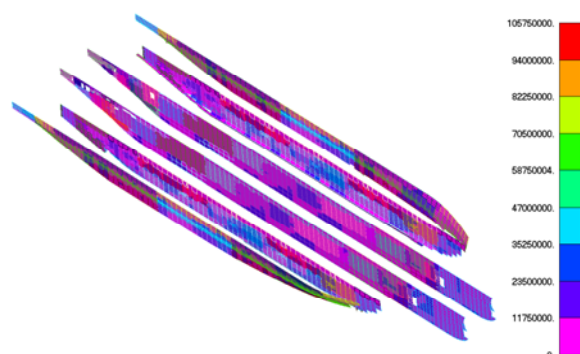


Figure 13: Shear stress in longitudinal HTV members for the static condition

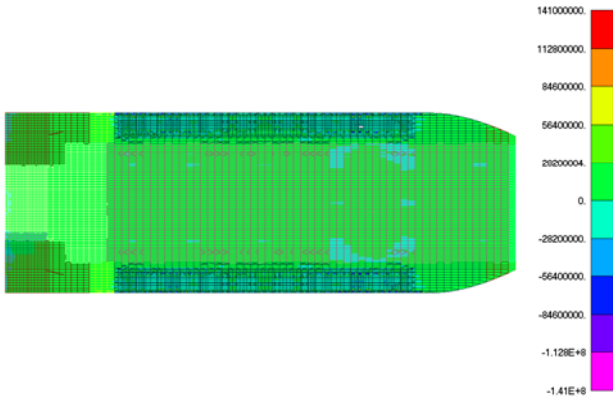


Figure 14: Bending stress in main deck of HTV for the static condition

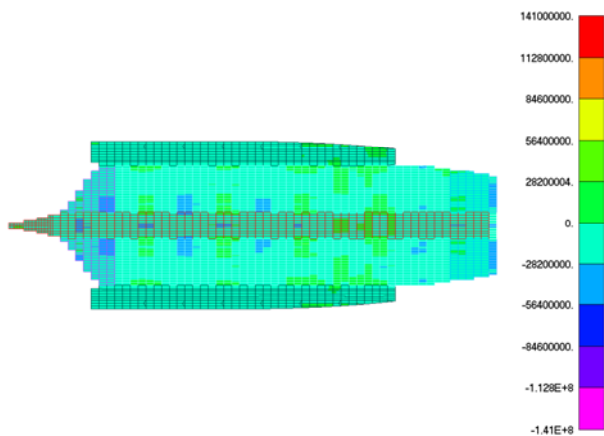


Figure 15: Bending stress in HTV bottom hull for the static condition

Based on test 1 it is concluded that stiffness interaction has a negligible influence on the maximum shear force and bending moment since the values for both methods are equal.

Benefit of the GHA method is that the shear distribution over the longitudinal members in transverse direction of the HTV is calculated while for the rigid-body method it is assumed to be equally distributed. Furthermore with the GHA method actual dynamic situations are assessed while the conventional rigid-body method takes a percentage of the total capacity into account for the dynamic behaviour of the HTV independent of actual wave loads.

2.3 (e) HTV deflection validations

For certain projects, vessel deflections are of importance for cargo and/or seafastening. Furthermore it can be used to determine whether uplift will occur. Since head- or following waves will result in the largest vessel deflections, this wave heading is considered in both methods.

To calculate vessel deflections, the conventional GHS method uses the following assumptions:

- Wave length = vessel length (lpp)
- Wave height = max wave height = $1.86 * H_{sig}$

Based on above mentioned assumptions, a static analysis is performed. In 12 steps the wave top is moved along the vessel length to calculate the deflection at certain phases. The deflection is calculated assuming the following:

- Vessel is a beam with a certain cross-section
- Static analysis, no accelerations

From the integrated FE model used for the GHA, also the deflection of the vessel can be determined. In contradiction to the GHS method, the GHA uses:

- Realistic wave length determined by the spectral analysis
- Dynamic analysis including accelerations
- Transverse/torsional deflections can be determined using the GHA results

Figures 16 & 17 present a comparison between the HTV vertical deflections for both methods.

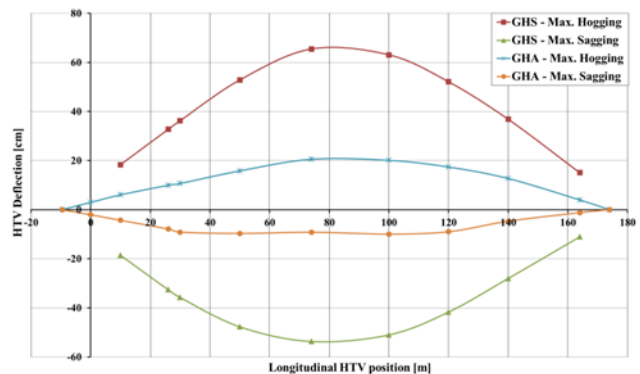


Figure 16: HTV deflection comparison between GHA & GHS for test case 1

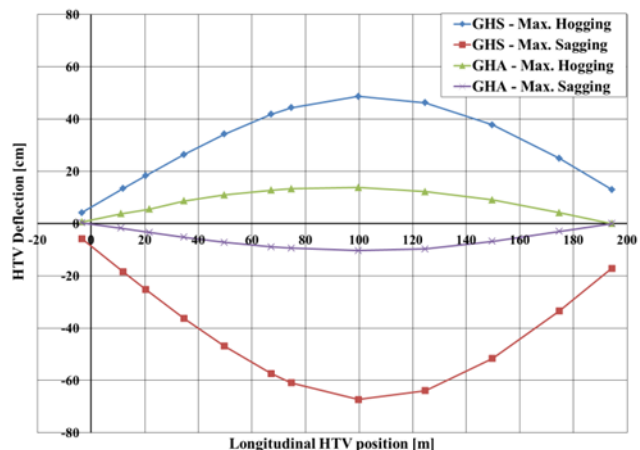


Figure 17: HTV deflection comparison between GHA & GHS for test case 2

The same trend in deflections is recognized for both test cases; i.e. deflections calculated by the conventional GHS method are more severe than for the GHA method.

Reason why these deflections are more severe has mainly to do with the assumptions taken for the GHS method. Especially the wave length has significant impact on the deflections. Because it is not known for the rigid-body method which wave length is most severe, a worst case wave length is assumed.

Another reason why the deflections are lower for the GHA method has to do with stiffness interaction. Especially for test case 2, stiffness of the cargo has a significant contribution to the overall stiffness of the system, which mainly visible in the sagging condition. Due to the stiffness of the cargo, deflections in sagging condition are significantly lower.

It is concluded that the deflections calculated with the GHS method are more severe than the ones calculated with the GHA method due to:

- Applied wave
- Stiffness interaction

2.4 CONCLUSION & RECOMMENDATIONS

Overall it is concluded that the more detailed GHA method to determine the design criteria is required in the following cases:

- Critical transports in the conventional rigid-body method calculations
- Large overhanging cargo
- Expectation that stiffness of cargo has significant impact on the design criteria like cribbing load

It is recommended to compare the results of more transports with each other to find out whether a trend could be obtained from the results. In future it could increase safety and save resources when general knowledge from the GHA could be applied to all transports.

3. OPERATIONAL IMPROVEMENTS

An overview is given on the methods used within Dockwise to generate the design wave height for heavy marine transports. Operational insights are given and the increased amount of data, compared to [2], is analysed, shown and reviewed. In addition a prognosis is given about future developments to come to a design wave height based on the measured weather data.

3.1 DESIGN WAVE HEIGHT DETERMINATION

This paragraph gives an overview of three different methods to derive the design wave height for heavy transport voyages.

3.1 (a) Standard design method

As a standard design method the scatter diagrams from the Global Wave Statistics are used at Dockwise. From these available wave statistics the short term design sea state is derived where the significant wave height has a probability of exceedance of 5% for

the most severe area. Given the season and the transit time through the area, the probability of exceedance of the individual “3-hour stationary storm” design wave height is calculated. To account for calm periods the calculation is corrected for wave smaller than 4.0 [m]. Reference is made to Dockwise guidelines and criteria [3] for detailed description about the design wave height determination.

Wave height relaxation in non-head sea conditions may be considered for vessels with redundant propulsion systems. According to the Noble Denton Guidelines for marine operations [6] a vessel with a redundant propulsion system is defined as having, as a minimum:

- 2 or more independent main engines
- 2 or more independent fuel supplies
- 2 or more independent power transmission systems
- 2 or more independent switchboards
- 2 or more independent steering systems, or an alternative means of operation of a single steering system (but excluding emergency steering systems that cannot be operated from the bridge)
- The ability to maintain any desired heading in all condition up to and including the design storm, taking into account the wind age of the cargo.

The maximum reduction of design wave height is given in Table 3.

Table 3: directional wave height relaxation Noble Denton

<i>Dir wrt bow [deg]</i>	<i>% of design wave height</i>
30 / 0 / 330	100
45 / 315	90
60 / 300	80
75 / 285	70
90 / 270	60
105 / 255	70
120 / 240	80
135 / 225	90
150 / 180 / 210	100

3.1 (b) Short trip scenario

In a very limited number of cases, where vessels are not redundant or where accelerations due to bow/stern waves result in unacceptable forces to the cargo, a short trip scenario could be used to reduce the design wave height. This method is only to be used if enough safe havens exist along the planned route. In addition extensive safety precautions are to be taken when a short trip scenario is included in the design. Weather forecast need to be obtained from 2 different providers and it is advisable to provide dedicated route forecast by a specialized company.

3.1 (c) SafeTrans

The MARIN program SafeTrans is an integrated tool to design marine heavy lift transports in a safe and efficient manner using state of the art analysis methods, databases, and hydrodynamics. This DNV approved software includes the master’s decisions to avoid adverse weather and uses Monte Carlo simulations based on a hind cast/fore cast database. By using the knowledge and experience of the master in the design the wave height can be reduced. In addition an estimate is given on the amount of weather delays. Reference is made to Aalbers et al [5].

3.2 OPERATIONAL INSIGHTS

The theoretical methods to determine the design wave height and accelerations are evaluated by using full scale weather forecast and motion measurements. Reference is made to [2] for a detailed description on the Octopus motion monitoring system as installed on all Dockwise vessels. The latest results are presented from the Octopus system and insights are given with respect to using nowcast weather data, influence of the angle of loll and overhang of cargo.

3.2 (a) Nowcast versus Design wave height

An update is given about the nowcast wave height registrations from the Dockwise vessels. As recommended in [2] the significance of this research has increased from 55 to 140 voyages and from 530.000 nm to 1.178.292 nm, see Figure 23. It is important to investigate if the presented conclusions are still valid.

The logged GPS position is used to determine which Areas according the GWS are crossed during each transport. The nowcast significant wave height is compared to the design wave height for each area of a voyage. From the nowcast wind and swell waves a total wave height per time step is determined by taking the quadratic sum of both waves. Results of the wave height comparison are shown in Figure 18. The following formula is used to determine the non-dimensional $\delta_{\text{nowcast_Design}}$.

$$\delta_{\text{Nowcast_Design}} = \frac{\text{nowcast}}{\text{Design}}$$

Figure 18 shows that the design wave height was almost never exceeded according to the recorded nowcast wave height from SPOS. At 4 points the Nowcast wave height was slightly exceeded. Looking to the maximum recorded nowcast significant wave height of 5.0 [m] our masters have been able to avoid larger forecasted waves. This is an interesting conclusion because it shows that our masters avoid regions where the forecast wave height is larger than 4.5-5.0 [m]. This graph validates the DW/Anglo Eastern policy about avoiding heavy weather for HTV’s. In addition there is a time factor which avoids vessels ending up in excessive waves, in the order of 9 to 10 [m], which typically need some time to build up and hence are better predictable in

advance. Please note that the actual wave height could have been larger when the forecast underestimated the weather.

Figure 18 also shows that with increasing design wave height the operational margin increases. While the lowest operational margin occurs at 3.0-5.0 [m] significant design wave height, the $\delta_{\text{nowcast_Design}}$ for higher design sea states reduces to values smaller than 60%. This trend is traced back to the fact that master’s decisions about routing and bad weather avoidance increase the operational margin at larger design waves. Generally speaking it is shown that design waves larger than 5.0 [m] are never encountered for the analysed voyages in this database.

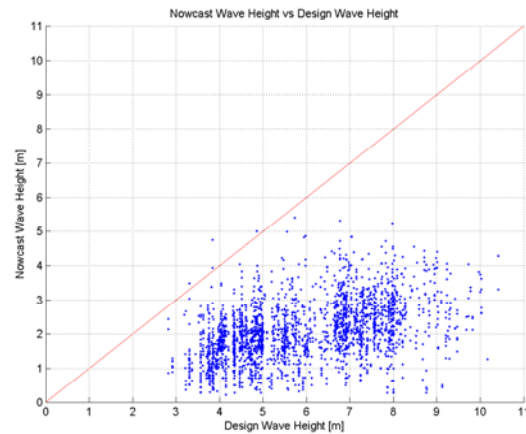


Figure 18: nowcast significant wave height vs. Design wave height per Area according to GWS

3.2 (b) Measured versus design accelerations

In order to exclude any uncertainty of weather data and the conversion from weather data to motion data, the focus is transferred to measured accelerations. The measured acceleration is compared to a single design acceleration value, which is determined with Shipmo for each voyage. Reference is made to Dockwise Guidelines and Criteria [4] for a detailed description on ship motion calculations by Shipmo. The following formula is used to determine the non-dimensional $\delta_{\text{Measured_Design}}$ to be able to compare multiple transports.

$$\delta_{\text{Measured_Design}} = \frac{\text{Measured}}{\text{Design}}$$

The number of occurrences versus the value of this δ gives important information on the actual operational margin during heavy transports. The total number of 3-hour occurrences, as plotted in Figures 19 to 22 is 31980, which is around 4000 sailing days of different Dockwise vessels.

Figures 19 and 20 are presented to focus on measured longitudinal, x and transverse, y accelerations in the cargo CoG compared to design accelerations. These figures show that the operational margin increases with increasing design acceleration. This conclusion confirms the conclusion from the Nowcast wave data.

Another interesting conclusion is that the operational margin for x acceleration is smaller than the operational margin for y acceleration. This conclusion confirms that during heavy weather the master turns his vessel into bow waves. The determination of the design pitch motion and y acceleration could also influence this conclusion, because of usage of the strip theory with limited accuracy for longitudinal motions i.e. surge and pitch.

It should also be kept in mind that x acceleration is generally much smaller than y acceleration. Design accelerations are used to determine seafastening forces between vessel and cargo. As x accelerations are generally small and cribbing friction is significant, the seafastening force is often replaced by a minimum of 5% of the cargo weight, which increases the operational margin. This additional safety margin is not displayed in these graphs because measured and design accelerations are compared directly and thus show the operational margin.

Figure 20 shows also that two measured acceleration points for y acceleration were almost 100% of the design. Please note that for that particular voyage wave height relaxation was used in order to keep the acceleration within limits for cargo strength. The seafastening forces were calculated with non reduced wave heights in order to maintain equal safety standards for all transports. The conclusion is that this practice reduces the operational margin as shown in this Figure. In addition one point exceeds the design acceleration with 50%, as a result of large overhang and low stability. Reference is made to paragraph 3.2 (d) for review of this voyage.

Several conclusions are drawn from Figure 21 and 22, which display for x and y acceleration the $\delta_{\text{Measured_Design}}$ number of 3-hour occurrences. For x and y acceleration the average $\delta_{\text{Measured_Design}}$ is around 0.1375 and 0.125 respectively. Next to this it can be seen that only a small number of occurrences is larger than 50% of the design value. For x and y direction the probability of 3-hour occurrences larger than 50% is 2.84% and 2.15% respectively.

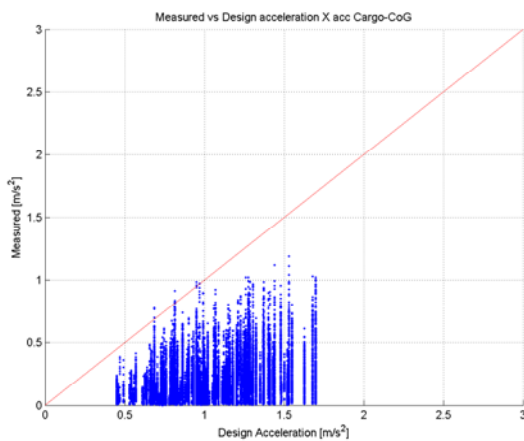


Figure 19: X acceleration Measured vs. Design

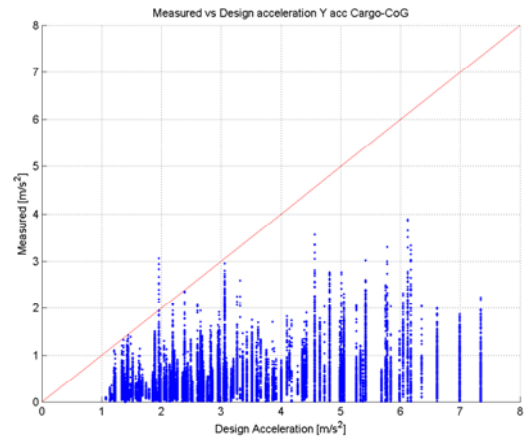


Figure 20: Y acceleration Measured vs. Design

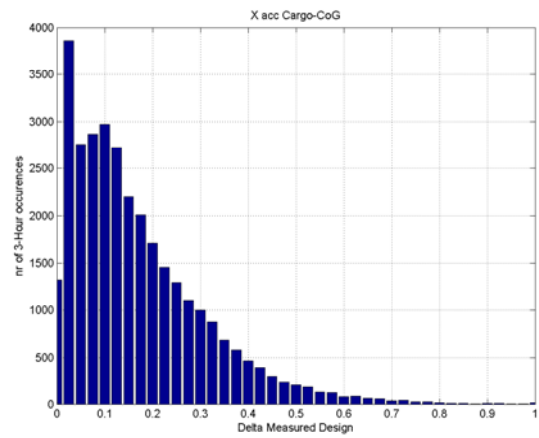


Figure 21: X acc in Cargo CoG occurrences vs $\delta_{\text{Measured_Design}}$

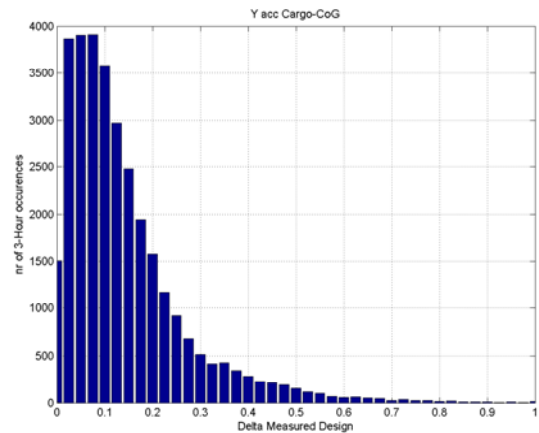


Figure 22: Y acc in Cargo CoG occurrences vs $\delta_{\text{Measured_Design}}$

3.2 (c) Wind influences on accelerations

For transports with a large cargo windage area like jack-up rigs, the wind speed could have effect on the measured transverse acceleration. In the transport design analysis the wind contribution is split in two parts, a static wind force and a force due to the angle of loll. It is to be noted that the forces from the wind are included in the seafastening load, but the transverse acceleration

from the angle of loll is not included in the design acceleration as presented in the CSM. However the measured accelerations include both the effects of wave and wind induced motions.

From the analysed voyages some examples exist where the angle of loll was 4-7 degrees. In one case the $g \cdot \sin(\phi)$ term from the angle of loll was larger than the transverse acceleration from the wave induced motions. To include this effect the transverse design accelerations are corrected for the wind angle of loll for three voyages.

3.2 (d) effect of cargo overhang on accelerations

In the heavy transport it is not unusual to sail with buoyant overhang of cargo in the order of 20 [m]. Generally this has little or no effect on the ship motions. However it is found from a couple of transports that the effect on ship motions could be large. The ideal recipe that leads to small transverse design accelerations and large chance of exceeding these is the following combination:

- large buoyant overhang
- low GM
- large roll period > 35 [s], outside wave spectrum
- low freeboard
- large angle of loll

Due to the small stability, a small exciting force is enough to result in a roll angle of several degrees. Depending on the actual loading condition and configuration waves of a couple of meters could cause the vessel to roll and let the overhang touch the water. This suddenly gives an increase in stability, which results in unexpected ship motions that were not taken into account in the design process. One transport out of the 140 show that transverse design accelerations are exceeded with 50%, while seastate did not reached the design value.

It is not easy to include these effects in the frequency domain ship motion analysis due to their non-linear character. Internal research was performed to use a 3D diffraction program, but this did not yet lead to an accurate method. Additional damping and excitation terms cause difficulties in calculating accurate motion analysis without performing model tests.

Model tests with overhang of a large semi submersible show also that when waves hit the bottom of the cargo and if there is significant submergence the transverse accelerations increase. This increase could be up to 35% compared to ship motions obtained from the linear theory.

It is important to note that for the above described topic the transports were still safe because the minimum seafastening capacity is defined to be 5-10% of the (large) cargo weight by the Marine warranty surveyors. In addition the steel to wood friction coefficient is generally set to 0.2 while model tests show that 0.4 or even 0.5 is a more realistic value.

3.3 OPERATIONAL BASED DESIGN METHOD

A research project is started to investigate how the data can contribute to a more realistic and safer design wave height method. The aim is to reach a constant operational margin by increasing the design sea-state at the lower range and reducing the design sea-state at the higher range. Marine warranty surveyors are also interested in the design of this new method and have offered to contribute to the project.

At the moment of writing tools are available to produce GWS Area and Season specific wave scatter diagrams from the SPOS nowcast data, see Figure 24. The black numbers are produced from the Octopus Nowcast data and the red numbers are generated by GWS observations. The figure shows again lower significant wave height. In addition the mean T_z from the diagram is also lower. An interesting question is how the Octopus wave scatter diagrams could be used as input for a new design wave height method.

Preliminary calculations are performed to generate a design wave height based on equal probability of exceedance compared to the standard design method by using a Weibull fit. The maximum nowcast wave height is registered to be 5.5 [m], which causes that this method cannot be used directly for standard design wave heights of 7-8 [m] or larger.

Other questions that arise are how the wind and swell waves should be combined in one scatter diagram. Large differences are present between wave periods and wave directions, which can have a large effect on the vessel motions. Would it be possible to generate separate wind and swell scatter diagrams as input for ship motion analysis and combine the results afterwards?

3.4 CONCLUSIONS & RECOMMENDATIONS

With almost 1.200.000 nm of ship motion and weather data the significance of the research project has increased and the conclusion are still standing and valid. In addition it shows clear justification to design a operational based method to determine a more realistic design wave height at the higher sea states.

It is proposed to keep working on collecting data from the fleet to further increase the statistics and significance.

Operational insights are given on the effects of wind contribution and cargo overhang. Both topics can have significant impact on the ship motions in particular circumstances.

Further investigation is scheduled to design an operational based method for the design wave height determination where masters decision to avoid adverse weather are included. This could lead to a more realistic and safer heavy transport design.

4. CONCLUSIONS & RECOMMENDATIONS

Both theoretical and operational improvements lead to more insight in heavy marine transportation. It is valuable to improve the calculation methods to increase knowledge and insight about transporting larger and heavier structures. It is recommended to keep working on improvements and to compare results from different voyages to see if trends exist and if standards and quick calculations method could be improved.

5. REFERENCES

1. O.A.J. Peters and L.J.M. Adegeest, 'Motion Monitoring and Decision Support during Heavy Transport', OMAE2010- 21143, 2010.
2. J.B. de Jonge and O.A.J. Peters, 'Operational margin from weather and motion database for heavy transport vessels', OMAE2011-49811, 2011.
3. DOCKWISE GC.ENG101 "Routing and Design Environmental Conditions", *Guidelines and Criteria*, November 2008.

4. DOCKWISE GC.ENG.302 "Motion Response Analysis", *Guidelines and Criteria*, November 2008.
5. A.B. Aalbers, "A new software system for safer rig moves", Marin, Safetrans technical notes.
6. GL Noble Denton, "Guidelines for Marine operations 0030/ND", Sect 7.2.10, 31 March 2010.

6. AUTHORS BIOGRAPHY

Martijn van Exsel holds the position of structural engineer at Dockwise. He is involved in all kind of strength related topics like vessel/cargo strength verifications and design of supports/grillages and all other non-custom requirements.

Jan de Jonge works as a marine engineer at Dockwise and is involved in all kind of hydromechanics topics like ship motion behaviour, mooring, environment and model testing. In addition daily work involves leading a fleet wise motion monitoring project, processing and analysing of the data.

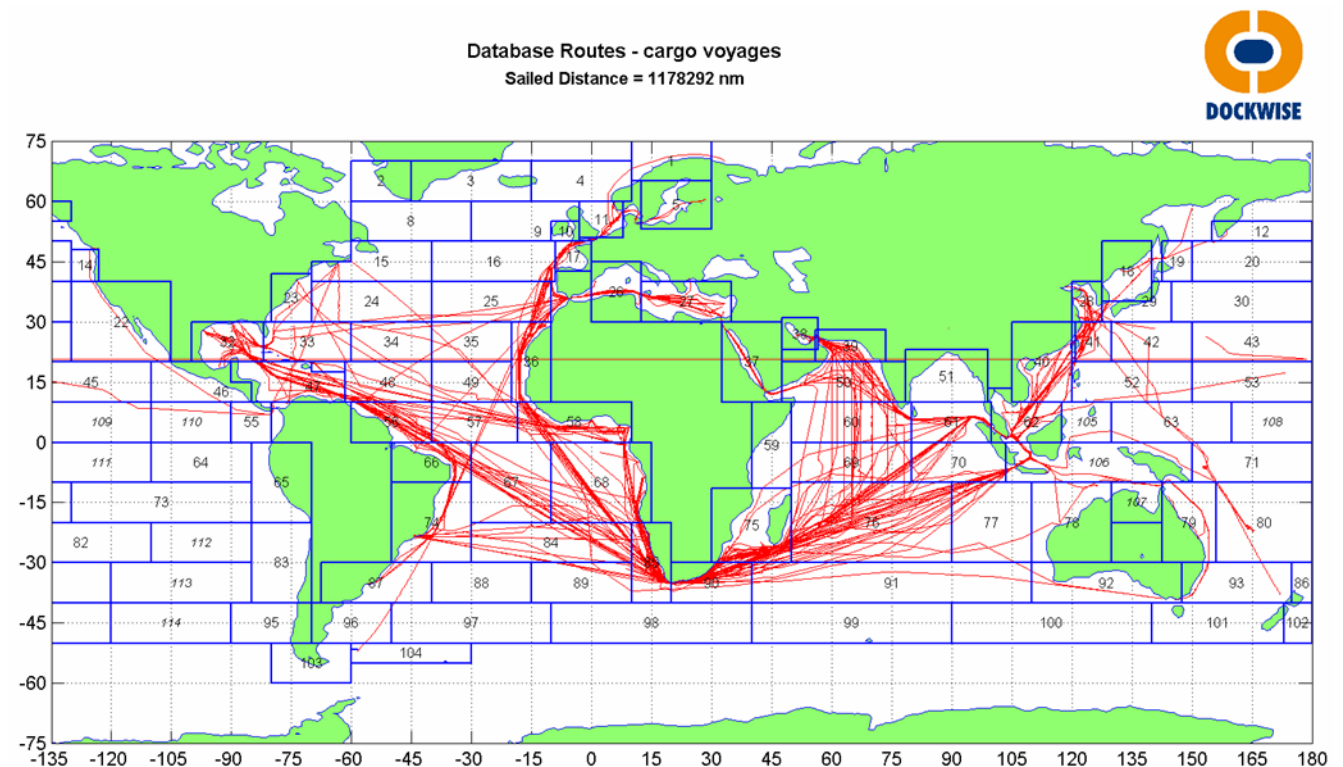


Figure 23 sailed routes of DW heavy transport vessels.



combined scatter diagram cargo
 year, area 90
 Based on 2439 3-hour observations
 all wave directions

Hs(m)	<4	4.5	5.5	6.5	7.5	8.5	9.5	10.5	11.5	12.5	>13	sum	P(Hsig)
sum	39 ⁰	84 ²	141 ²⁷	228 ¹²¹	266 ²⁴⁷	163 ²⁵²	60 ¹⁹⁶	15 ¹⁰⁰	3 ⁴⁰	0 ¹²	0 ⁴	1000 ¹⁰⁰⁰	0.0000
15	0 ⁰	0 ⁰	0 ⁰	0 ⁰	0 ⁰	0 ⁰	0 ⁰	0 ⁰	0 ¹	0 ⁰	0 ⁰	0 ¹	0.9995
14	0 ⁰	0 ⁰	0 ⁰	0 ⁰	0 ⁰	0 ⁰	0 ⁰	0 ⁰	0 ¹	0 ⁰	0 ⁰	0 ¹	0.9995
13	0 ⁰	0 ⁰	0 ⁰	0 ⁰	0 ⁰	0 ⁰	0 ⁰	0 ¹	0 ¹	0 ⁰	0 ⁰	0 ¹	0.9995
12	0 ⁰	0 ⁰	0 ⁰	0 ⁰	0 ⁰	0 ⁰	0 ⁰	0 ¹	0 ¹	0 ⁰	0 ⁰	0 ²	0.9995
11	0 ⁰	0 ⁰	0 ⁰	0 ⁰	0 ⁰	0 ⁰	0 ¹	0 ¹	0 ¹	0 ⁰	0 ⁰	0 ³	0.9995
10	0 ⁰	0 ⁰	0 ⁰	0 ⁰	0 ⁰	0 ¹	0 ¹	0 ²	0 ¹	0 ¹	0 ⁰	0 ⁵	0.9995
9	0 ⁰	0 ⁰	0 ⁰	0 ⁰	0 ⁰	0 ¹	0 ³	0 ³	0 ¹	0 ¹	0 ⁰	0 ⁹	0.9995
8	0 ⁰	0 ⁰	0 ⁰	0 ⁰	0 ¹	0 ³	0 ⁵	0 ⁴	0 ²	0 ¹	0 ¹	0 ¹⁶	0.9995
7	0 ⁰	0 ⁰	0 ⁰	0 ⁰	0 ²	0 ⁶	0 ¹⁰	0 ⁸	0 ⁴	0 ²	0 ¹	0 ³³	0.9995
6	0 ⁰	0 ⁰	0 ⁰	0 ¹	1 ⁷	1 ¹⁴	0 ²⁰	0 ¹⁴	0 ⁶	0 ²	0 ¹	2 ⁶⁵	0.9986
5	0 ⁰	0 ⁰	0 ⁰	2 ⁴	7 ¹⁸	3 ³²	2 ³⁶	0 ²¹	0 ⁸	0 ³	0 ¹	15 ¹²³	0.9905
4	1 ⁰	2 ⁰	9 ¹	19 ¹²	53 ⁴⁶	29 ⁶⁰	20 ⁵³	10 ²⁵	3 ⁸	0 ²	0 ⁰	145 ²⁰⁹	0.9079
3	2 ⁰	14 ⁰	62 ⁴	141 ³⁵	169 ⁸⁷	115 ⁸⁴	37 ⁵⁰	5 ¹⁸	0 ⁵	0 ¹	0 ⁰	546 ²⁸³	0.4960
2	32 ⁰	66 ¹	70 ¹³	66 ⁵⁶	36 ⁷⁷	15 ⁴⁸	1 ¹⁷	0 ⁴	0 ²	0 ⁰	0 ⁰	286 ²¹⁸	0.0481
1	4 ⁰	2 ²	0 ⁸	0 ¹⁴	0 ⁸	0 ²	0 ⁰	0 ⁰	0 ⁰	0 ⁰	0 ⁰	7 ³⁵	0.0026

Figure 24 nowcast scatter diagram recorded along the sailed route, black is Octopus, red is GWS.